The Journal of Immunology

Purinergic P2X7 Receptor Drives T Cell Lineage Choice and Shapes Peripheral γδ Cells

Michela Frascoli, Jessica Marcandalli, Ursula Schenk and Fabio Grassi

J Immunol 2012; 189:174-180; Prepublished online 30 May 2012;
doi: 10.4049/jimmunol.1101582
http://www.jimmunol.org/content/189/1/174

The Journal of Immunology is published twice each month by The American Association of Immunologists, Inc., 1451 Rockville Pike, Suite 650, Rockville, MD 20852

Print ISSN: 0022-1767 Online ISSN: 1550-6606.

Purinergic P2X7 Receptor Drives T Cell Lineage Choice and Shapes Peripheral γδ Cells

Michela Frascoli,* Jessica Marcandalli,* Ursula Schenk,*,[1] and Fabio Grassi*,[†]

TCR signal strength instructs αβ versus γδ lineage decision in immature T cells. Increased signal strength of γδTCR with respect to pre-TCR results in induction of the γδ differentiation program. Extracellular ATP evokes physiological responses through purinergic P2 receptors expressed in the plasma membrane of virtually all cell types. In peripheral T cells, ATP released upon TCR stimulation enhances MAPK activation through P2X receptors. We investigated whether extracellular ATP and P2X receptors signaling tuned TCR signaling at the αβ/γδ lineage bifurcation checkpoint. We show that P2X7 expression was selectively increased in immature γδ$^+$CD25$^+$ cells. These cells were much more competent to release ATP than pre–TCR-expressing cells following TCR stimulation and Ca^{2+} influx. Genetic ablation as well as pharmacological antagonism of P2X7 resulted in impaired ERK phosphorylation, reduction of early growth response (*Egr*) transcripts induction, and diversion of γδTCR-expressing thymocytes toward the αβ lineage fate. The impairment of the ERK-Egr-inhibitor of differentiation 3 (Id3) signaling pathway in γδ cells from *p2rx7*$^{-/-}$ mice resulted in increased representation of the Id3-independent NK1.1-expressing γδ T cell subset in the periphery. Our results indicate that ATP release and P2X7 signaling upon γδTCR expression in immature thymocytes constitutes an important costimulus in T cell lineage choice through the ERK-Egr-Id3 signaling pathway and contributes to shaping the peripheral γδ T cell compartment. *The Journal of Immunology*, **2012, 189: 174–180.**

Productive rearrangement of gene segments at *Tcrβ*, *Tcrγ*, and *Tcrδ* loci is instrumental in T cell development in the thymus. The protein products of these stochastic recombination events, the pre-TCR (constituted by the rearranged TCRβ-chain in covalent association with the invariant pre–TCRα-chain) (1) and γδTCR, influence the thymocyte to commit to the αβ and γδ lineage, respectively (2). Whereas differentiation of γδ T cells is generally characterized by lack of expression of CD4 and CD8 coreceptor molecules (3, 4), development of αβ T cells is characterized by the transition of thymocytes through an ordered sequence of phenotypes defined by the expression of CD4 and CD8. Cells progress from the most immature CD4$^-$8$^-$ double-negative (DN) stage to the mature either CD4$^+$8$^-$ or CD4$^-$8$^+$ single positive (SP) stage through an intermediate CD4$^+$8$^+$ double-positive (DP) stage. The DN stage can be further subdivided according to the expression of CD25 and CD44 with maturation characterized phenotypically by the following sequence: CD44$^+$25$^-$ (DN1) > CD44$^+$25$^+$ (DN2) > CD44$^-$25$^+$ (DN3) > CD44$^-$25$^-$ (DN4) (5). In particular, the DN3 stage is a fundamental checkpoint at which pre-TCR and γδ TCR signals instruct commitment to αβ and γδ lineage, respectively (6). β-Selection is associated with higher CD5 and CD27 expression and increase in cell size, which define the DN3b stage (7, 8). Two elegant studies have shown that TCR signal strength rather than TCR signal quality determines lineage choice, a strong TCR signal resulting in γδ and a weak signal in αβ commitment. In fact, attenuation of γδTCR signal strength or expression level induced differentiation of γδTCR-expressing thymocytes along the αβ pathway to the DP stage (9, 10). Whether concomitant costimuli contribute to TCR signal strength in γδ lineage choice is at present unknown. In addition, differential signaling by the γδTCR can result in development of γδ NKT cells, which express NK.1.1 and, in contrast with conventional γδ cells, are relatively independent from the ERK-early growth response (Egr)-inhibitor of differentiation 3 (Id3) signaling axis.

We have previously shown that signal transduction by the TCR in peripheral CD4 T cells determines the increase in ATP synthesis and the release through calcium-sensitive pannexin-1 hemichannels, which in turn activates in an autocrine fashion purinergic P2X receptors (ATP-gated nonselective cationic channels) in the plasma membrane. This signaling loop acts as a costimulus for MAPK signaling and implements cell cycling as well as IL-2 secretion (11, 12). Pioneering experiments have shown that immature thymocytes are responsive to extracellular ATP through P2X receptors (13). Rearrangement competent but not incompetent DN3 thymocytes undergo spontaneous cytosolic Ca^{2+} oscillations, which might lead to ATP release. We tested whether ATP released as a result of pre-TCR and/or γδTCR expression affected thymocyte differentiation through P2X receptors signaling. We show that P2X7 receptor activation contributes to γδTCR signal strength and that genetic ablation as well as pharmacological antagonism of P2X7 diverts γδTCR-expressing cells toward the αβ fate. Moreover, impaired γδTCR signaling in *p2rx7*$^{-/-}$ mice resulted in increased representation of Id3-independent NK1.1$^+$ TCR Vδ6.3$^+$ cells in the periphery.

*Institute for Research in Biomedicine, CH-6500 Bellinzona, Switzerland; and [†]Dipartimento di Biologia e Genetica per le Scienze Mediche, Università degli Studi di Milano, I-20133 Milano, Italy

[1]Current address: Pharmanalytica SA, Locarno, Switzerland.

Received for publication June 2, 2011. Accepted for publication April 28, 2012.

This work was supported by Grant 310030-124745 from the Swiss National Science Foundation, Grant KFS 02445-08-2009 from the Swiss Cancer League, the Fondazione Ticinese per la Ricerca sul Cancro, the Fondazione Leonardo, the AGD Italia (Coordinamento Associazioni Italiane Giovani con Diabete), Leo Club Italia, and the Sixth Research Framework Program of the European Union, Project MUGEN (MUGEN LSHG-CT-2005-005203) (to F.G.).

Address correspondence and reprint requests to Dr. Fabio Grassi, Institute for Research in Biomedicine, Via Vincenzo Vela 6, CH-6500 Bellinzona, Switzerland. E-mail address: fabio.grassi@irb.usi.ch

The online version of this article contains supplemental material.

Abbreviations used in this article: BzATP, benzoyl-ATP; DN, double-negative; DP, double-positive; Egr, early growth response; ERK, extracellular signal regulated kinase; FTOC, fetal thymic organ culture; Id3, inhibitor of differentiation 3; oATP, periodate-oxidized ATP; OP9-DL1, OP9 BM stromal cell transduced with the Notch ligand Delta-like 1; SP, single-positive; WT, wild-type.

www.jimmunol.org/cgi/doi/10.4049/jimmunol.1101582

Materials and Methods

Mice

C57BL/6 (wild-type [WT]) mice were obtained from Charles River Laboratories Germany and *p2rx7*$^{-/-}$ (14), and *rag1*$^{-/-}$ C57BL/6 mice were obtained from The Jackson Laboratory. Mice were used at 4 wk to isolate thymocytes and at 8 wk to analyze γδ cells in peripheral tissues. The animals were bred and treated in accordance with the Swiss Federal Veterinary Office guidelines and were kept in specific pathogen-free animal facility.

Flow cytometry and cell culture

For FACS analysis, mAbs conjugated with biotin, FITC, PE, PerCP, PerCP-Cy5.5, PE-Cy7, allophycocyanin, or allophycocyanin-Cy7 against the following Ags were used: CD8a (53-6.7), CD4 (L3T4), CD25 (PC61.5), CD44 (IM7), CD27 (LG.7F9), CD3ε (145-2C11), TCRβ (H57-597), TCRγ/δ (GL3) (eBioscience); TCR Vγ2 (UC3-10A6), TCR Vδ6.3/2 (8F4H7B7) (BD Biosciences); and TCRVγ3 (536) and TCR Vδ4 (552143) (BioLegend). All samples were acquired with a FACSCanto (BD Biosciences) and analyzed with FlowJo software (Tree Star).

Thymi were homogenized and washed in RPMI 1640 medium containing 10% (v/v) FBS. In some cases, thymocyte samples were depleted of CD8$^+$ and CD4$^+$ cells by treatment with anti-CD8 (31.M) and anti-CD4 (RL172) mAbs with low-tox-M Rabbit Complement (Cederlane Laboratories). TCRδ$^-$ DN3a thymocytes were sorted as CD44$^-$CD25$^+$CD27^{low} and TCRδ$^-$ DN3b thymocytes as CD44$^-$CD25$^+$CD27^{high}. Thymocytes subsets were sorted with a FACSAria (BD Biosciences).

Sorted γδ$^+$CD25$^+$cells were plated onto subconfluent OP9 BM stromal cells transduced with the Notch ligand Delta-like 1 (OP9-DL1) monolayers previously subjected to gamma irradiation (40 Gy) at 5×10^4 cells/well in a 96-well plate. All cocultures were performed in the presence of 1 ng/ml IL-7 and 5 ng/ml Flt3 ligand (PeproTech) in α-MEM containing 20% (v/v) FBS. When indicated, plates were coated with mAb specific for TCRδ (clone 3A10; final concentration, 10 μg/ml) before OP9 cells were plated. OP9-DL1 cells were maintained as described previously (15). Where indicated, periodate-oxidized ATP (oATP) (Medestea) and A438079 (Tocris Bioscience) at 200 μM as a selective P2X7 inhibitor were added.

For analysis of the extent of phosphorylation of ERK, sorted γδ$^+$CD25$^+$ cells (5×10^4 cells/well) were stimulated for 16 h with the indicated stimuli, permeabilized, and incubated with rabbit mAbs against phosphorylated ERK (Thr^{202}/Tyr^{204}) (D13.14.4E) (Cell Signaling Technology).

Real-time PCR

Total RNA was isolated with TRIzol reagent (Invitrogen) and then reverse transcribed to generate cDNA with random hexamer primers and a Moloney murine leukemia virus reverse transcriptase kit (Invitrogen). To quantify transcripts, we treated mRNA samples with 2 U DNase (Applied Biosystems) per sample. Transcripts were quantified by real-time quantitative PCR on an ABI PRISM 7700 Sequence Detector with predesigned TaqMan Gene Expression Assays and reagents according to the manufacturer's instructions (Perkin-Elmer/Applied Biosystems). Probes with the following Applied Biosystems assay identification numbers were used: *p2rx1* (Mm00435460_m1), *p2rx2* (Mm01202369_g1), *p2rx3* (Mm00523699_m1), *p2rx4* (Mm00501787_m1), *p2rx5* (Mm00473677_m1), *p2rx7* (Mm00440582_m1), *Egr1* (Mm00656724_m1), *Egr2* (Mm00456650_m1), *Egr3* (Mm00516979_m1), and *Rn18s* (EUK 18S rRNA [DQ] Mix). For each sample, mRNA abundance was normalized to that of 18S rRNA and is presented in arbitrary units.

Ca^{2+} imaging and measurement of ATP release

Sorted thymocytes were loaded for 30 min at room temperature with 5 μM Fura-2 pentacetoxy-methylester in α-MEM, washed in the same solution, and plated on a monolayer of OP9-DL1 or OP9-GFP cells previously seeded on poly-L-lysine–coated coverslips. Coverslips were then washed and transferred to the recording chamber of an inverted microscope (Axiovert 200; Zeiss) equipped with an Andor 885 JCS iXON classic camera. For Ca^{2+} measurements, Polychrome V (Till Photonics) was used as a light source. After excitation at 340 and 380 nm, the emitted light was acquired at 505 nm. The sampling rate was 1 Hz. Ca^{2+} concentrations are expressed as the 340/380 fluorescence ratio. The experiments were performed in a static modified Krebs–Ringer solution (155 mM NaCl, 4.5 mM KCl, 10 mM glucose, 5 mM Hepes [pH 7.4], 1 mM $MgCl_2$, and 2 mM $CaCl_2$) at 28–30°C. To inhibit TCR signaling in DN3 thymocytes, the src-like kinase inhibitor PP2 (VWR International) was used at 10 μM.

ATP release was measured by means of a two-enzyme assay, as described previously (16). Briefly, cells were plated on poly-L-lysine–coated coverslips, which were fixed in the recording chamber of an inverted microscope. Cells were incubated in modified Krebs–Ringer solution supplemented with 8 U/ml each of hexokinase and glucose 6-phosphate dehydrogenase and 5 mM NADP. In the presence of ATP, these enzymes catalyze the formation of NADPH, a fluorescent molecule that was visualized using fluorescence microscopy with an excitation wavelength of 340 nm and an emission at 460 nm. The fluorescence intensity of regions on or outside the cells was measured using TILLvisION software, and ATP concentrations were estimated using ATP standard solutions of known concentrations.

For measurement of cellular ATP, cells were lysed in 1% Triton X-100 and frozen on dry ice until analyzed with the ATP determination kit (Molecular Probes).

Fetal thymus organ culture

The medium for fetal thymus organ culture (FTOC) was IMDM plus GlutaMAX medium with 20% (v/v) FBS, 50 μM 2-ME, 1 mM sodium pyruvate, penicillin, and streptomycin. WT or *p2rx7*$^{-/-}$ fetal thymic lobes at E14 were cultured for various times in FTOC medium on isopore membrane filters (Millipore) and then were analyzed by flow cytometry. Cultures were provided fresh medium every 2 d.

Statistical analysis

Statistical analysis was performed with the Student *t* test. Data are reported as means ± SEM or SD. The *p* values <0.05 were considered significant ($*p < 0.05$, $**p < 0.01$, $***p < 0.001$).

Results

TCR-dependent Ca^{2+} oscillations, ATP synthesis, and release in immature thymocytes

We labeled sorted DN3 thymocytes from WT and *rag1*$^{-/-}$ C57BL/6 mice with Fura-2 and analyzed them for cytosolic Ca^{2+} variations in live imaging. Because Notch signaling is required for survival of DN3 cells (17) and pre–TCR-driven transition to the DP stage (18, 19), we cocultured DN3 cells with OP9-DL1 (15). Thymocytes from WT mice displayed spontaneous Ca^{2+} oscillations. In contrast, recombinase deficiency resulted in complete absence of spontaneous calcium waves, indicating that expression of pre-TCR and/or γδTCR was required for cytosolic Ca^{2+} elevations (Fig. 1A). Calcium spikes detected in WT thymocytes were also observed by coculturing WT cells with nontransduced OP9 cells. No significant differences were observed both in percentage of responding cells and in number of Ca^{2+} elevations per cell between thymocytes cocultured with OP9-DL1 and DL1-null OP9 cells, thereby suggesting that calcium oscillations were not dependent on Notch activation (Supplemental Fig. 1A, 1B). Because γδTCR signaling in immature γδ thymocytes and progression along the γδ developmental pathway are independent from Notch signaling relative to the Notch dependent pre-TCR signaling, these results suggest that γδTCR induces cytosolic Ca^{2+} elevations in immature thymocytes. Accordingly, the percentage of cells displaying Ca^{2+} elevations was dramatically reduced by treatment with PP2, which inhibits src-like (e.g., lck/fyn) tyrosine kinase activity, suggesting that increases in cytosolic Ca^{2+} were dependent on most proximal signaling by γδTCR and possibly pre-TCR (Fig. 1B).

We have previously shown that cytosolic Ca^{2+} increases in T cells determines ATP release through Ca^{2+}-sensitive pannexin-1 hemichannels (11). We compared ATP release in TCRδ$^-$CD27$^+$ DN3b cells (>97% TCRβ$^+$) and CD25$^+$TCRδ$^+$ cells upon exposure to the ionophore ionomycin to provoke massive Ca^{2+}-sensitive release of ATP. This treatment resulted in robust ATP release by γδ but not pre–TCR-expressing DN3b cells and CD27$^-$ DN3a cells (Fig. 2A), thereby suggesting that expression of the γδTCR induces Ca^{2+} dependent enhanced ATP release in the developing

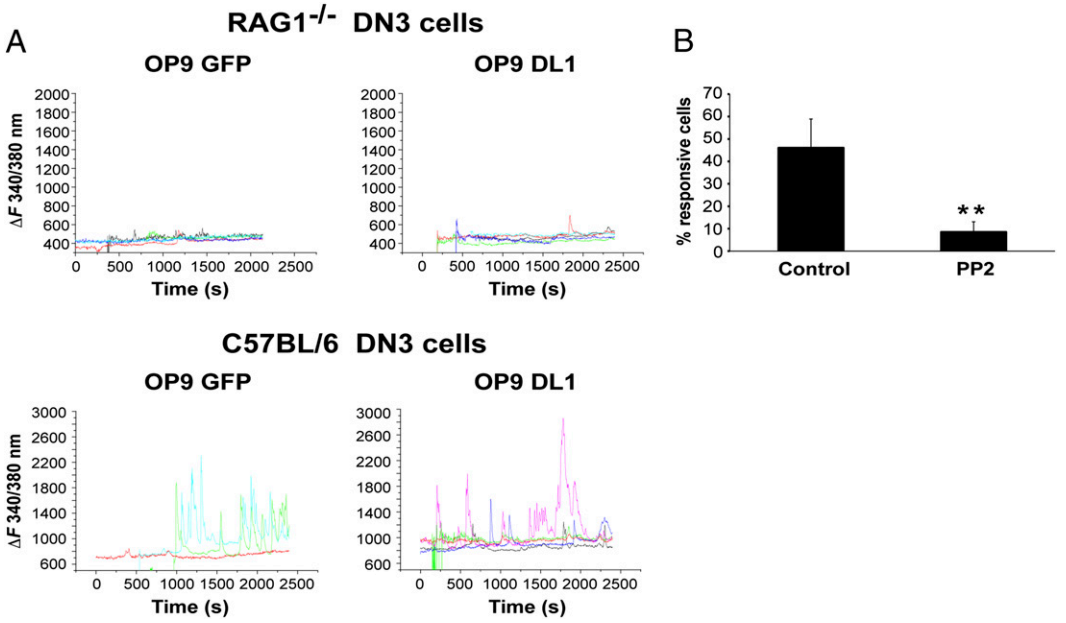

FIGURE 1. Ca^{2+} signaling in DN3 thymocytes. (**A**) Representative cytosolic Ca^{2+} profiles of DN3 thymocytes from the indicated mice in coculture with OP9-GFP or OP9-DL1 monolayers. Cytosolic Ca^{2+} elevations were detected in RAG-1–proficient cells independently of Notch ligand expression by cocultured stromal cells. Number of cells analyzed were C57BL/6 on OP9-DL1, 60; C57BL/6 on OP9-GFP, 40; *rag1*$^{-/-}$ on OP9-DL1, 115; and *rag1*$^{-/-}$ on OP9-GFP, 75 (see Supplemental Fig. 1 for statistics). (**B**) Percentages of DN3 thymocytes displaying Ca^{2+} oscillations either in medium or in the presence of 10 μM PP2. Data are cumulative of three independent experiments, $n = 76$ (control), 188 (PP2); $^{**}p < 0.01$.

T cell. To see whether pre-TCR and γδTCR signaling differently affected ATP levels in immature DN thymocytes, we measured intracellular ATP increases upon stimulation with anti-CD3 mAb in CD25^{+}TCRδ^{+}, DN3a, and DN3b cells. Fig. 2B shows that γδTCR signaling in CD25^{+} cells induced significantly increased intracellular ATP levels with respect to pre-TCR. Moreover, ATP release could be readily measured upon stimulation with anti-CD3 mAb-coated beads in CD25^{+}TCRδ^{+} (Fig. 2C) but not DN3a and DN3b thymocytes (Supplemental Fig. 1C) by a two-enzyme assay in live-cell imaging experiments (16). Altogether, these results indicate that γδTCR in immature thymocyte is a more potent inducer of ATP synthesis and release than the pre-TCR, and is

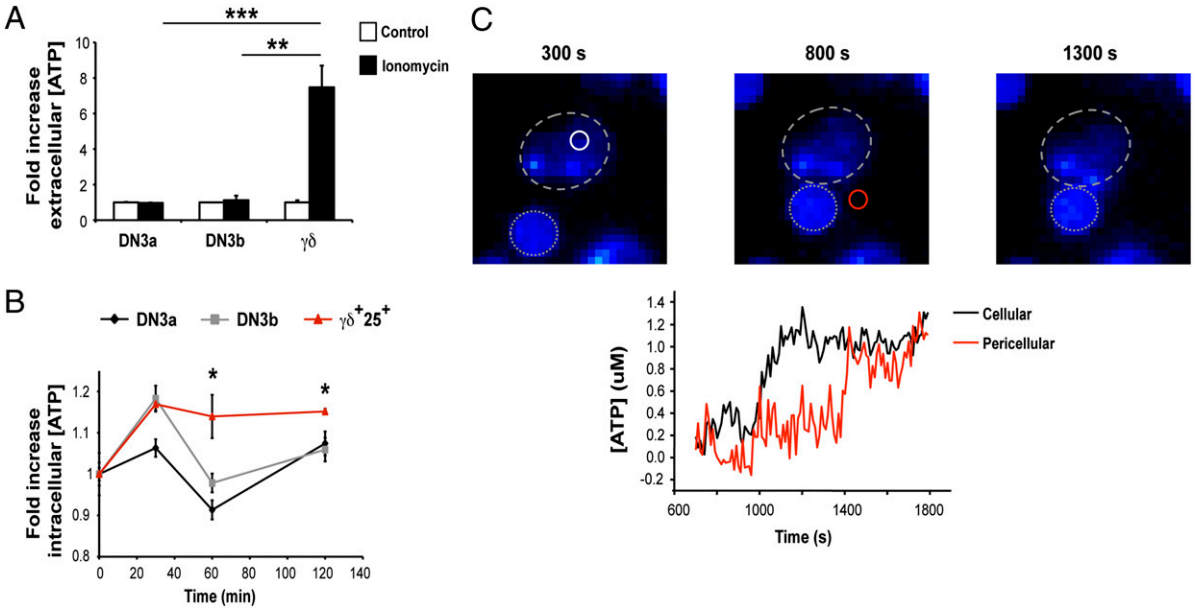

FIGURE 2. ATP production and release in DN3 and immature γδ thymocytes. (**A**) Histograms representing ionomycin-induced release of ATP in the supernatant of DN3a, DN3b, and γδ^{+}CD25^{+} thymocytes. Data are representative of three independent experiments. $^{**}p < 0.01$; $^{***}p < 0.001$; $n = 5$. (**B**) Fold increase in the concentration of cytosolic ATP in sorted DN3a, DN3b, and γδ^{+}CD25^{+} cells from WT mice at different time points after T cell activation with anti-CD3 Abs. Data are representative of three independent experiments. $^{*}p < 0.05$; $n = 3$. (**C**) ATP release from γδ^{+}CD25^{+} cells stimulated with CD3 mAb-coated beads was measured as an increase in NADPH fluorescence generated by a two-enzyme assay. Pseudocolor images and ATP levels in a region of interest placed above the cell (black line) or in proximity of the same cell (red line) show the increase in pericellular fluorescence. The fluorescence increase over the cell body is indicative of calcium-induced mitochondrial NADPH synthesis. Original magnification ×40. In the present experiment, 27 cells were monitored.

responsible of enhanced purinergic signaling in the γδTCR expressing cells.

Expression of purinergic P2X receptors during T cell development

Analysis of P2X transcripts by real-time PCR at different stages of T cell development in the thymus revealed the higher expression of *p2rx4* and *p2rx7* genes at the DN and CD4 SP stages (Fig. 3A). We did not test *p2rx6* because its transcript was not detectable in any thymocyte subset (data not shown). To get insight into transcriptional regulation of *p2rx4* and *p2rx7* genes in the DN compartment during αβ and γδ lineage commitment, we sorted DN3a and DN3b cells as well as immature $CD25^+$ γδTCR cells and analyzed transcription of *p2rx* genes by real-time PCR. This experiment revealed the selective expression of *p2rx7* in $\gamma\delta^+CD25^+$ cells (Fig. 3B).

P2X7-mediated regulation of γδ T cell lineage commitment

To see whether P2X7 contributed to lineage choice of γδTCR-expressing immature thymocytes, we performed FTOC with E14 thymi from $p2rx7^{-/-}$ embryos. Analysis of thymocyte subsets for CD4 and CD8 expression revealed no differences in the distribution of thymocytes as DN, DP, and SP cells (Fig. 4A) as well as DN1 to four subsets defined by CD44 and CD25 expression (Supplemental Fig. 1D). However, $p2rx7^{-/-}$ FTOC showed the significant increase of γδTCR-expressing DP cells both as percentage and absolute number (Fig. 4B), suggesting that lack of P2X7 signaling caused the aberrant transition of γδTCR-expressing cells to an αβ-lineage like DP stage. Then, we performed FTOC with WT E14 thymi in the presence of oATP, a pharmacological P2X antagonist (20). Also, in the presence of oATP DP cells expressing TCRδ chains were significantly increased (Fig. 4C), suggesting aberrant αβ commitment of γδTCR-expressing cells by pharmacological P2X antagonism. To more specifically address the contribution of P2X7 in γδ commitment, we performed FTOC from both C57BL/6 and BALB/c embryos in the presence of the selective P2X7 antagonist A438079. These experiments revealed the significant decrease of γδ DN cells ($p < 0.001$) as well as the significant increase of γδ DP cells ($p < 0.001$) in both strains (Supplemental Fig. 2). In addition, we addressed the effect of oATP on γδ cell differentiation by coculturing $\gamma\delta^+CD25^+$ cells with OP9-DL1 cells in the presence of γδTCR mAb, which implements the differentiation of $CD25^+$ γδTCR-bearing cells to the DN mature stage (6). These experiments confirmed the aberrant transition of $\gamma\delta^+$ cells to the DP stage in the presence of oATP in a dose-dependent fashion (Fig. 4C). Finally, to show that P2X7 signaling contributes to γδ commitment, we performed FTOC in the presence of the selective P2X7 agonist benzoyl-ATP (BzATP) (21). Whereas BzATP did not influence the development of TCRβ-expressing cells (Supplemental Fig. 1E), it determined the significant increase of γδ cells in the DN compartment (Fig. 4D), suggesting that P2X7 stimulation promoted the acquisition of the mature DN phenotype by γδTCR-bearing cells. A polymorphism in the cytoplasmic domain of P2X7, which expresses either a proline (found in BALB/c mice) or leucine (present in C57BL/6 mice) at position 451 confers high and low sensitivity to stimulation, respectively (22). Consistent with increased P2X7 activity in BALB/c mice, 6-d FTOC from E14 embryos revealed the significant increase in γδ cells development in BALB/c versus C57BL/6 cultures (Fig. 5A).

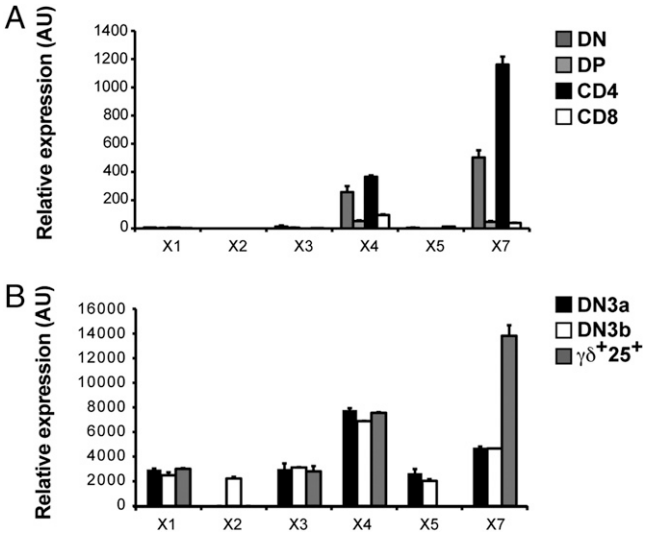

FIGURE 3. Expression of P2X receptors in thymocyte cell subsets. (**A**) Representative experiment showing P2X receptors expression by quantitative real-time PCR on cDNA from DN, DP, $CD4^+$, and $CD8^+$ SP thymocyte subsets. (**B**) Transcriptional regulation of purinergic receptors during T cell development at the DN stage by real-time PCR. Mean values of triplicates ± SD from a single experiment representative of three are shown. AU, arbitrary unit.

Extracellular ATP and P2X7 signaling contribute to TCR signal strength in γδ lineage commitment

P2X7 expression in cells otherwise devoid of P2X7 increases intracellular ATP content and supports cell growth through P2X7 stimulation by secreted ATP (23). Analysis of intracellular ATP levels following CD3 stimulation of γδ thymocytes showed lack of ATP increase in $p2rx7^{-/-}$ with respect to WT cells (Fig. 6A). We have previously shown that reduced ATP levels in $p2rx7^{-/-}$ regulatory T cells correlated with reduced ERK phosphorylation compared with the WT counterpart (24). Attenuation of ERK phosphorylation was shown to divert γδ thymocytes to the αβ lineage (9, 10). Then, we addressed whether P2X7 expression affected ERK phosphorylation in $\gamma\delta^+CD25^+$ thymocytes cocultured with OP9-DL1 cells. $P2rx7^{-/-}$ γδ cells displayed impaired phospho-ERK and cell size increases after 16-h stimulation with TCRδ mAb. These effects were also observed in WT γδ thymocytes upon addition of oATP (Fig. 6B). Altogether, our results point to a role of P2X7 in tuning TCR signal strength in γδ lineage commitment. Accordingly, *egr1*, *egr2*, and *egr3* transcripts, which are controlled by γδTCR signal strength (9), were diminished in ex vivo-purified $p2rx7^{-/-}\gamma\delta^+CD25^+$ thymocytes with respect to WT cells (Fig. 6C).

Impact of P2X7 activity on peripheral γδ T cells

We investigated whether *p2rx7* deletion affected the γδ cells peripheral pool. We did not detect significant differences in total γδ cells in peripheral lymph nodes, uterus, and lungs from 8-wk-old $p2rx7^{-/-}$ and WT mice. However, γδ cells were significantly decreased in mesenteric lymph nodes from $p2rx7^{-/-}$ mice (Supplemental Fig. 3). Peripheral γδ cells are heterogeneous and can be distinguished by expression of TCRs using distinct TCRγ and TCRδ variable (V) regions. For example, expression of TCRVδ4 characterizes principally cells in the intestinal epithelium, spleen, thymus, and lactating mammary glands. This cell subset was not differently represented in the thymus, spleen, and mesenteric lymph nodes from $p2rx7^{-/-}$ and WT mice (data not shown). The defect of ERK signaling we observed in developing $p2rx7^{-/-}$ γδ cells should affect the ERK-Egr-Id3 signaling axis, which is required for the development of cells expressing TCR Vγ4 and Vγ5 (according to Heilig and Tonegawa nomenclature; Refs. 25 and 26). Cells expressing TCR Vγ4 were not significantly different in

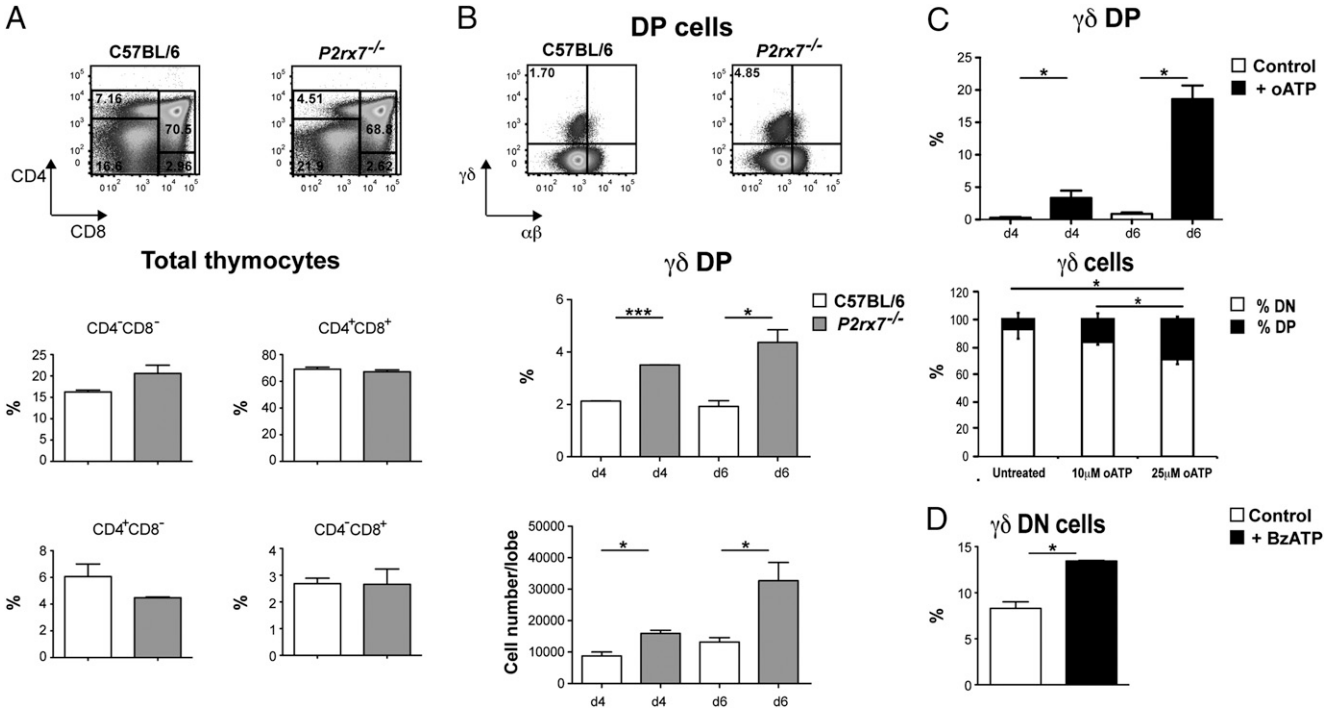

FIGURE 4. Effect of *p2rx7* genetic deletion and pharmacological P2X antagonism on γδ T cell development. (**A**) Dot-plot analysis of thymocytes from E14 WT and $p2rx7^{-/-}$ thymi after 4 d FTOC stained with CD4 and CD8 mAb. Histograms indicate percentage ± SD of the indicated thymocyte subsets after 4 d FTOC. Data are cumulative of five independent experiments. (**B**) Dot-plot analysis of thymocytes gated on DP cells from E14 WT and $p2rx7^{-/-}$ thymi after 6 d FTOC stained with TCRβ and TCRδ mAbs. Histograms representing percentages (*top panel*) and absolute numbers (*bottom panel*) of γδ cells in the DP compartment in WT and $p2rx7^{-/-}$ FTOC at days 4 and 6 of culture. Data are cumulative of five independent experiments. $*p < 0.05$; $***p < 0.001$. (**C**) Histograms representing percentage of γδ DP cells at days 4 and 6 in WT FTOC either untreated or treated with 100 μM oATP (*top panel*). Data are cumulative of five independent experiments. $*p < 0.05$. Histograms representing the percentage of DP and DN cells after 5 d coculture of $γδ^+CD25^+$ cells on OP9-DL1 cells with the addition of the indicated concentration of oATP (*bottom panel*). Data are representative of three independent experiments. $*p < 0.05$; $n = 3$. (**D**) Statistical analysis of γδ DN thymocytes from E14 WT thymi after 4 d FTOC in the presence of 150 μM BzATP. Data are cumulative of three independent experiments. $*p < 0.05$.

the spleen and lungs; however, they were significantly reduced in mesenteric lymph nodes of 8-wk-old $p2rx7^{-/-}$ mice, and cells expressing TCR Vγ5 were dramatically reduced in the uterus of $p2rx7^{-/-}$ females (Supplemental Fig. 4). Consistent with increased P2X7 activity in BALB/c mice, we detected a significant increase of γδ cells expressing TCR Vγ4 in BALB/c lymph nodes with respect to C57BL/6 mice (Fig. 5B). These results suggest that signaling by P2X7 substantially contributes to the development of the γδ T cells peripheral pool that depends on the ERK-Egr-Id3 axis.

Lack of Id3 provokes an outgrowth of cells expressing TCR Vγ1 and Vδ6.3 together with the NK cells marker NK1.1, referred to as γδ NKT cells (27). Consistent with an impairment of the ERK-Egr-Id3 pathway in developing γδ cells from $p2rx7^{-/-}$ mice, we detected a significant increase in $NK1.1^+$ cells expressing Vδ6.3/2 in the uterus (Fig. 7) and Peyer's patches albeit nonsignificant

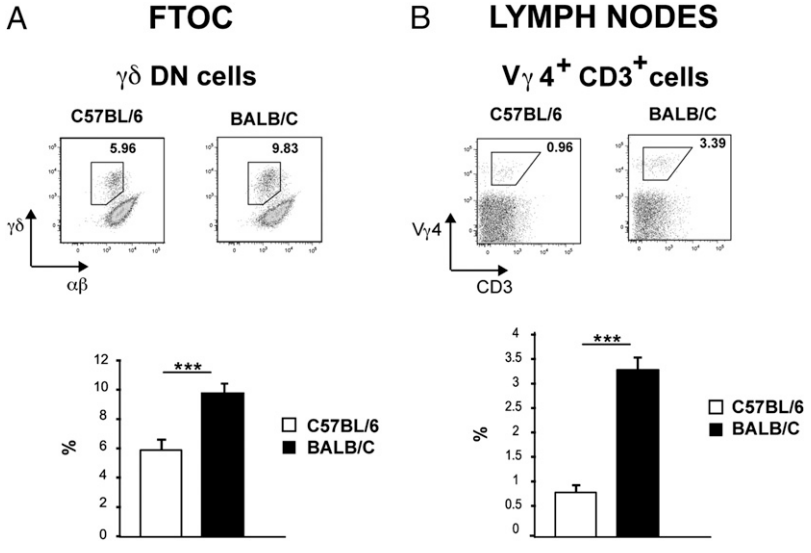

FIGURE 5. Enhanced γδ T cells development and peripheral representation in BALB/c mice. (**A**) Dot-plot analysis of electronically gated DN thymocytes from E14 C57BL/6 and BALB/c thymi after 6 d FTOC stained with TCRβ and TCRδ mAbs. Histograms indicate percentage ± SD of DN γδ cells. Data are cumulative of six independent experiments. (**B**) Dot-plot analysis of lymph node cells from C57BL/6 and BALB/c mice stained with TCRVγ4 and CD3 mAbs. Histograms indicate percentage ± SD of $TCRVγ4^+CD3^+$ cells ($n = 6$). $***p < 0.001$.

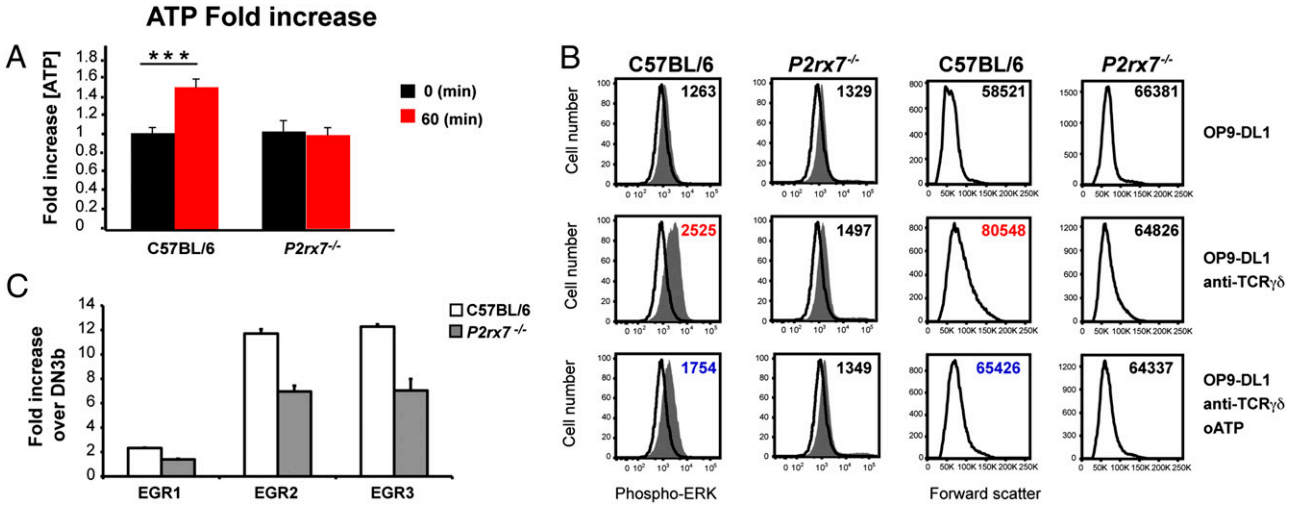

FIGURE 6. ATP synthesis, ERK phosphorylation, and *egr* induction in γδ$^+$CD25$^+$ thymocytes. (**A**) Changes in intracellular ATP concentration in WT and *p2rx7*$^{-/-}$ γδ$^+$CD25$^+$ cells at baseline (black bars) and after 60-min stimulation with anti-CD3 mAb (red bars). ***$p < 0.001$; $n = 5$. (**B**) Analysis in flow cytometry of ERK phosphorylation and forward scatter in γδ$^+$CD25$^+$ thymocytes cocultured with OP9-DL1 stromal cells either untreated or treated as indicated. Sixty-two percent and 70% inhibitions of ERK phosphorylation and cell size increase, respectively, were observed by oATP treatment in WT cells stimulated with anti-γδTCR (10 μg/ml) mAb. No variations in ERK phosphorylation and cell size increase were observed in *p2rx7*$^{-/-}$ cells upon anti-CD3 stimulation. A single experiment representative of three is shown. (**C**) Analysis of *egr1*, *egr2*, and *egr3* expression by real-time PCR on sorted γδ$^+$ CD25$^+$ cells isolated from WT and *p2rx7*$^{-/-}$ mice. Data are represented as fold increase over DN3b cells subset. Mean values of triplicates ± SD from a single experiment representative of three are shown. AU, arbitrary unit.

(data not shown) of 8-wk-old *p2rx7*$^{-/-}$ mice. Altogether, these observations point to a role of P2X7 activity in contributing to lineage choice in γδ T cell development and shaping of the peripheral pool of γδTCR-expressing cells.

Discussion

In 1997, Ross et al. (13) have shown that immature thymocytes are responsive to P2X7 agonists, and they hypothesized that extracellular ATP could act as a signal for growth and differentiation of DN thymocytes. DN3 thymocytes, which include γδ and αβ committed cells, showed Notch-independent but lck/fyn-dependent (e.g., TCR dependent) spontaneous Ca^{2+} oscillations. Cytosolic Ca^{2+} elevations in peripheral T cells determine ATP release through pannexin-1 hemichannels (11). Notably, we could measure ATP release in CD25$^+$ γδ but not pre–TCR-expressing DN3b cells upon exposure to the ionophore ionomycin. In addition, significant increases in intracellular ATP were observed in γδ versus pre–TCR-expressing cells upon CD3 stimulation, suggesting that γδTCR signaling determines enhanced ATP synthesis and release in the developing T cell.

Analysis of P2X transcripts by real-time PCR revealed higher expression of *p2rx7* in γδ$^+$CD25$^+$ cells. Then, we analyzed T cell development in FTOC with E14 thymi from *p2rx7*$^{-/-}$ embryos. Despite normal β selection, these experiments showed a significant increase of γδTCR-expressing DP cells, indicating that lack of P2X7 signaling favored the aberrant transition of γδTCR-expressing cells to the DP stage. This cell subset was observed in pTα-deficient mice in which thymus cellularity is dramatically reduced and the absence of the pre-TCR complex severely impairs the development of αβ T cells. Conversely, γδ lineage differentiation is not impaired, and γδTCR expression together with Notch could support development of DP αβ-lineage like cells (28). The αβ-lineage–like development observed in γδTCR-bearing *p2rx7*$^{-/-}$ thymocytes was observed also in WT cells by pharmacological P2X antagonism with oATP or selective inhibition of P2X7 by A438079 both in C57BL/6 and BALB/c FTOC. These data indicate that ATP/P2X signaling contributes to the acquisition of the physiological CD4$^-$8$^-$ γδ cells phenotype. Accordingly, FTOC performed in the presence of the prototypic P2X7 agonist, Bz-ATP, showed a significant increase of CD4$^-$8$^-$ γδ cells.

Attenuation of ERK phosphorylation induced by γδTCR signaling diverted γδ thymocytes to the αβ lineage differentiation pathway indicating that TCR signal strength was crucial in the acquisition of the CD4$^-$8$^-$ phenotype (9, 10). Because ATP/P2X signaling promotes ERK activation (24), we compared ERK phosphorylation in WT and *p2rx7*$^{-/-}$CD25$^+$ γδ cells upon TCR

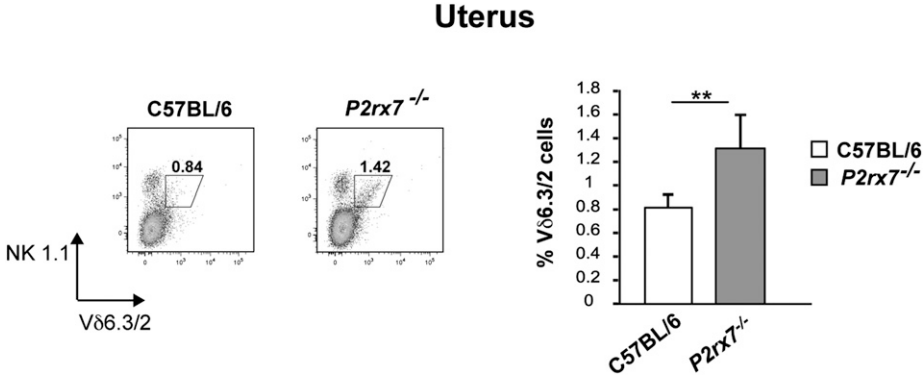

FIGURE 7. Analysis of NK1.1$^+$ γδ cells from uterus of WT and *p2rx7*$^{-/-}$ mice. Dot-plot analysis of cells obtained from WT and *p2rx7*$^{-/-}$ uterus stained with TCRVδ6.3/2 and NK1.1 mAbs. Histograms indicate percentage ± SD of TCRVδ6.3/2$^+$NK1.1$^+$ cells ($n = 6$). **$p <$ 0.005.

stimulation. *P2rx7*$^{-/-}$ γδ cells displayed impaired phospho-ERK and cell size increases after 16-h stimulation with TCRδ mAb, an indication of the contribution of P2X7 to γδTCR signaling in CD25^{+} γδ cells. In addition, P2X7 expression determined an increase in ATP synthesis upon TCR stimulation likely through an autocrine feed-forward loop, as already observed in regulatory T cells (24). These results point to a role of P2X7 in tuning TCR signal strength in T cell development at the αβ/γδ lineage bifurcation checkpoint. Thus, we propose a model whereby ATP released by γδTCR signaling in immature thymocytes activates P2X receptors in an autocrine fashion and contributes to ERK phosphorylation as well as to implement the transcriptional program required for γδ T cell lineage commitment. In contrast with murine γδ cells, which differentiate independently from Notch, human γδ thymocytes depend on increased levels of Notch signaling than αβTCR-expressing cells (29). Human Notch activation might be interpreted as a stronger signal, thus conforming human T cell development to the TCR signal strength concept in T cell lineage commitment. In this respect, it would be interesting to see whether purinergic signaling contributes to TCR signal strength not only in murine but also in human T cell development.

Although the ERK-Egr-Id3 signaling axis plays a role in γδ lineage development, mice lacking Id3 display elevated numbers of γδ T cells (26, 30, 31). In fact, Id3-null mice have increased generation of "innate-like" γδ cells expressing TCR Vγ1.1 Vδ6.3 with limited junctional diversity. This γδ T cell subset shares phenotypic and functional characteristics with αβ NKT cells (27) and is repressed by Id3 (30, 31). In line with a role of P2X7 activity in the ERK-Egr-Id3 signaling pathway, *p2rx7*$^{-/-}$ mice displayed increased peripheral representation of this cell subset, suggesting a role of extracellular ATP in modulating γδ NKT cell development.

Acknowledgments

We thank Juan Carlos Zúñiga-Pflücker for providing OP9-GFP and OP9-DL1 cells, David Jarrossay for cell sorting, and Enrica Mira Catò for technical assistance with mice.

Disclosures

The authors have no financial conflicts of interest.

References

1. Groettrup, M., K. Ungewiss, O. Azogui, R. Palacios, M. J. Owen, A. C. Hayday, and H. von Boehmer. 1993. A novel disulfide-linked heterodimer on pre-T cells consists of the T cell receptor β chain and a 33 kd glycoprotein. *Cell* 75: 283–294.
2. Burtrum, D. B., S. Kim, E. C. Dudley, A. C. Hayday, and H. T. Petrie. 1996. TCR gene recombination and αβ-γδ lineage divergence: productive TCR-β rearrangement is neither exclusive nor preclusive of γδ cell development. *J. Immunol.* 157: 4293–4296.
3. Kang, J., M. Coles, D. Cado, and D. H. Raulet. 1998. The developmental fate of T cells is critically influenced by TCRγδ expression. *Immunity* 8: 427–438.
4. Passoni, L., E. S. Hoffman, S. Kim, T. Crompton, W. Pao, M. Q. Dong, M. J. Owen, and A. C. Hayday. 1997. Intrathymic δ selection events in γδ cell development. *Immunity* 7: 83–95.
5. Godfrey, D. I., J. Kennedy, T. Suda, and A. Zlotnik. 1993. A developmental pathway involving four phenotypically and functionally distinct subsets of CD3^{-} CD4^{-}CD8^{-} triple-negative adult mouse thymocytes defined by CD44 and CD25 expression. *J. Immunol.* 150: 4244–4252.
6. Kreslavsky, T., A. I. Garbe, A. Krueger, and H. von Boehmer. 2008. T cell receptor-instructed αβ versus γδ lineage commitment revealed by single-cell analysis. *J. Exp. Med.* 205: 1173–1186.
7. Taghon, T., M. A. Yui, R. Pant, R. A. Diamond, and E. V. Rothenberg. 2006. Developmental and molecular characterization of emerging β- and γδ-selected pre-T cells in the adult mouse thymus. *Immunity* 24: 53–64.
8. Hoffman, E. S., L. Passoni, T. Crompton, T. M. Leu, D. G. Schatz, A. Koff, M. J. Owen, and A. C. Hayday. 1996. Productive T-cell receptor β-chain gene rearrangement: coincident regulation of cell cycle and clonality during development in vivo. *Genes Dev.* 10: 948–962.
9. Haks, M. C., J. M. Lefebvre, J. P. Lauritsen, M. Carleton, M. Rhodes, T. Miyazaki, D. J. Kappes, and D. L. Wiest. 2005. Attenuation of γδTCR signaling efficiently diverts thymocytes to the αβ lineage. *Immunity* 22: 595–606.
10. Hayes, S. M., L. Li, and P. E. Love. 2005. TCR signal strength influences αβ/γδ lineage fate. *Immunity* 22: 583–593.
11. Schenk, U., A. M. Westendorf, E. Radaelli, A. Casati, M. Ferro, M. Fumagalli, C. Verderio, J. Buer, E. Scanziani, and F. Grassi. 2008. Purinergic control of T cell activation by ATP released through pannexin-1 hemichannels. *Sci. Signal.* 1: ra6.
12. Yip, L., T. Woehrle, R. Corriden, M. Hirsh, Y. Chen, Y. Inoue, V. Ferrari, P. A. Insel, and W. G. Junger. 2009. Autocrine regulation of T-cell activation by ATP release and P2X7 receptors. *FASEB J.* 23: 1685–1693.
13. Ross, P. E., G. R. Ehring, and M. D. Cahalan. 1997. Dynamics of ATP-induced calcium signaling in single mouse thymocytes. *J. Cell Biol.* 138: 987–998.
14. Solle, M., J. Labasi, D. G. Perregaux, E. Stam, N. Petrushova, B. H. Koller, R. J. Griffiths, and C. A. Gabel. 2001. Altered cytokine production in mice lacking P2X(7) receptors. *J. Biol. Chem.* 276: 125–132.
15. Schmitt, T. M., and J. C. Zúñiga-Pflücker. 2002. Induction of T cell development from hematopoietic progenitor cells by δ-like-1 in vitro. *Immunity* 17: 749–756.
16. Corriden, R., P. A. Insel, and W. G. Junger. 2007. A novel method using fluorescence microscopy for real-time assessment of ATP release from individual cells. *Am. J. Physiol. Cell Physiol.* 293: C1420–C1425.
17. Ciofani, M., and J. C. Zúñiga-Pflücker. 2005. Notch promotes survival of pre-T cells at the β-selection checkpoint by regulating cellular metabolism. *Nat. Immunol.* 6: 881–888.
18. von Boehmer, H., and H. J. Fehling. 1997. Structure and function of the pre-T cell receptor. *Annu. Rev. Immunol.* 15: 433–452.
19. Michie, A. M., and J. C. Zúñiga-Pflücker. 2002. Regulation of thymocyte differentiation: pre-TCR signals and β-selection. *Semin. Immunol.* 14: 311–323.
20. Murgia, M., S. Hanau, P. Pizzo, M. Rippa, and F. Di Virgilio. 1993. Oxidized ATP. An irreversible inhibitor of the macrophage purinergic P2Z receptor. *J. Biol. Chem.* 268: 8199–8203.
21. Young, M. T., P. Pelegrin, and A. Surprenant. 2007. Amino acid residues in the P2X7 receptor that mediate differential sensitivity to ATP and BzATP. *Mol. Pharmacol.* 71: 92–100.
22. Adriouch, S., C. Dox, V. Welge, M. Seman, F. Koch-Nolte, and F. Haag. 2002. Cutting edge: a natural P451L mutation in the cytoplasmic domain impairs the function of the mouse P2X7 receptor. *J. Immunol.* 169: 4108–4112.
23. Adinolfi, E., M. G. Callegari, D. Ferrari, C. Bolognesi, M. Minelli, M. R. Wieckowski, P. Pinton, R. Rizzuto, and F. Di Virgilio. 2005. Basal activation of the P2X7 ATP receptor elevates mitochondrial calcium and potential, increases cellular ATP levels, and promotes serum-independent growth. *Mol. Biol. Cell* 16: 3260–3272.
24. Schenk, U., M. Frascoli, M. Proietti, R. Geffers, E. Traggiai, J. Buer, C. Ricordi, A. M. Westendorf, and F. Grassi. 2011. ATP inhibits the generation and function of regulatory T cells through the activation of purinergic P2X receptors. *Sci. Signal.* 4: ra12.
25. Heilig, J. S., and S. Tonegawa. 1986. Diversity of murine γ genes and expression in fetal and adult T lymphocytes. *Nature* 322: 836–840.
26. Lauritsen, J. P., G. W. Wong, S. Y. Lee, J. M. Lefebvre, M. Ciofani, M. Rhodes, D. J. Kappes, J. C. Zúñiga-Pflücker, and D. L. Wiest. 2009. Marked induction of the helix-loop-helix protein Id3 promotes the γδ T cell fate and renders their functional maturation Notch independent. *Immunity* 31: 565–575.
27. Kreslavsky, T., A. K. Savage, R. Hobbs, F. Gounari, R. Bronson, P. Pereira, P. P. Pandolfi, A. Bendelac, and H. von Boehmer. 2009. TCR-inducible PLZF transcription factor required for innate phenotype of a subset of γδ T cells with restricted TCR diversity. *Proc. Natl. Acad. Sci. USA* 106: 12453–12458.
28. Fehling, H. J., A. Krotkova, C. Saint-Ruf, and H. von Boehmer. 1995. Crucial role of the pre–T-cell receptor α gene in development of αβ but not γδ T cells. *Nature* 375: 795–798.
29. Van de Walle, I., G. De Smet, M. De Smedt, B. Vandekerckhove, G. Leclercq, J. Plum, and T. Taghon. 2009. An early decrease in Notch activation is required for human TCR-αβ lineage differentiation at the expense of TCR-γδ T cells. *Blood* 113: 2988–2998.
30. Ueda-Hayakawa, I., J. Mahlios, and Y. Zhuang. 2009. Id3 restricts the developmental potential of γδ lineage during thymopoiesis. *J. Immunol.* 182: 5306–5316.
31. Verykokakis, M., M. D. Boos, A. Bendelac, E. J. Adams, P. Pereira, and B. L. Kee. 2010. Inhibitor of DNA binding 3 limits development of murine slam-associated adaptor protein-dependent "innate" γδ T cells. *PLoS ONE* 5: e9303.